**AUTHOR(S):** SARANYA, K., MOHAN, V., KIZEK, R., FERNANDEZ, C. and RAJENDRAN, L.

**TITLE:** Unprecedented homotopy perturbation method for solving nonlinear equations in the enzymatic reaction of glucose in a spherical matrix.

**YEAR:** 2018

**Publisher citation:** SARANYA, K., MOHAN, V., KIZEK, R., FERNANDEZ, C. and RAJENDRAN, L. 2018. Unprecedented homotopy perturbation method for solving nonlinear equations in the enzymatic reaction of glucose in a spherical matrix. Bioprocess and biosystems engineering [online], 41(2), pages 281-294. Available from: https://doi.org/10.1007/s00449-017-1865-0

**OpenAIR citation:** SARANYA, K., MOHAN, V., KIZEK, R., FERNANDEZ, C. and RAJENDRAN, L. 2018. Unprecedented homotopy perturbation method for solving nonlinear equations in the enzymatic reaction of glucose in a spherical matrix. Bioprocess and biosystems engineering, 41(2), pages 281-294. Held on OpenAIR [online]. Available from: https://openair.rgu.ac.uk

Bioprocess and Biosystems Engineering
https://doi.org/10.1007/s00449-017-1865-0

RESEARCH PAPER

# Unprecedented homotopy perturbation method for solving nonlinear equations in the enzymatic reaction of glucose in a spherical matrix

**K. Saranya[1] · V. Mohan[1] · R. Kizek[2,3] · C. Fernandez[4] · L. Rajendran[5]**

Received: 21 August 2017 / Accepted: 4 November 2017


## Abstract
The theory of glucose-responsive composite membranes for the planar diffusion and reaction process is extended to a microsphere membrane. The theoretical model of glucose oxidation and hydrogen peroxide production in the chitosan-aliginate microsphere has been discussed in this manuscript for the first time. We have successfully reported an analytical derived methodology utilizing homotopy perturbation to perform the numerical simulation. The influence and sensitive analysis of various parameters on the concentrations of gluconic acid and hydrogen peroxide are also discussed. The theoretical results enable to predict and optimize the performance of enzyme kinetics.

**Keywords** Enzyme-encapsulated polymer microspheres · Enzyme reaction mechanism · Mathematical modeling · New approaches of homotopy perturbation method

## Nomenclature

| | |
|---|---|
| $C_g$ | Concentration of glucose (mol/cm$^3$) |
| $C_{OX}$ | Concentration of oxygen (mol/cm$^3$) |
| $C_a$ | Concentration of gluconic acid:mol/cm$^3$ |
| $C_h$ | Concentration of hydrogen peroxide (mol/cm$^3$) |
| $D_g$ | Diffusion coefficient of glucose (cm$^2$/s) |
| $D_{OX}$ | Diffusion coefficient of oxygen (cm$^2$/s) |
| $D_a$ | Diffusion coefficient of gluconic acid (cm$^2$/s) |
| $D_h$ | Diffusion coefficient of hydrogen peroxide (cm$^2$/s) |
| $K_g$ | Michaelis–Menten constant for glucose:mol/cm$^3$ |
| $K_{OX}$ | Michaelis–Menten constant for oxygen (mol/cm$^3$) |
| $V_{max}$ | Maximal reaction velocity (cm/s) |
| $v_g$, $v_{OX}$, $v_a$ and $v_h$ | Stoichiometric coefficients (None) |
| $t$ | Time (S) |
| $C_g^*$ | Concentration of glucose in the external solution (mol/cm$^3$) |
| $C_{OX}^*$ | Concentration of glucose in the oxygen solution (mol/cm$^3$) |
| S | Radius of the microsphere ($\mu$m) |
| u | Dimensionless concentration of glucose (None) |
| v | Dimensionless concentration of oxygen (None) |
| w | Dimensionless concentration of gluconic acid (None) |
| H | Dimensionless concentration of hydrogen peroxide (None) |
| $\mathfrak{R}$ | Overall reaction rate (None) |
| T | Dimensionless time (None) |
| $\gamma_g$, $\gamma_{OX}$, $\gamma_a$, $\gamma_h$, $\alpha$ $\beta$ & $k$ | Dimensionless reaction diffusion parameters (None) |
| R | Dimensionless radius (None) |

**Electronic supplementary material** The online version of this article (https://doi.org/10.1007/s00449-017-1865-0) contains supplementary material, which is available to authorized users.

✉ L. Rajendran
raj_sms@rediffmail.com

1 Department of Mathematics, Thiagarajar College of Engineering Madurai, Madurai 625 015, India

2 Central Laboratories, Faculty of Pharmacy, University of Veterinary and Pharmaceutical Sciences Brno, Palackeho 1946/1, 612 42 Brno, Czech Republic

3 Department of Biomedical and Environmental Analyses, Wroclaw Medical University, Borowska 211, 50-556 Wroclaw, Poland

4 School of Pharmacy and Life Sciences, Robert Gordon University, Aberdeen AB107GJ,, UK

5 Department of Mathematics, Sethu Institute of Technology, Kariapatti 626115, India

Published online: 24 November 2017

## Introduction

Chemically reactive molecules which contain oxygen are defined as reactive oxygen species (ROS). Szatrowski et al. [1] discussed the production of large amount of hydrogen peroxide by human tumor cells. Superoxide, singlet oxygen, peroxides and hydroxyl radical are some examples of ROS. Over the past years the involvement of cancer with cellular oxidant stress and ROS has dramatically increased. This could be attributed to the high levels of ROS produced by cancer cells compared to normal cells in which different enzyme mechanisms form ROS. Different mathematical models have been suggested over the years in order to investigate the effect of enzymatic reaction with simultaneous diffusion.

Abdekhodaie et al. [2] reported a mathematical model to describe a dynamic process of diffusion of reactants, coupled with an enzymatic reaction inside a glucose composite membrane. Albin et al. [3] demonstrated a theoretical and experimental model of glucose-sensitive membrane. Rajendran and Bieniasz [4] analyzed the theoretical model of reaction and diffusion process in glucose-responsive composite membranes.

Recently, Abdekhodaie et al. [5] derived the mathematical equation to describe the kinetics of enzymes and the generation of hydrogen peroxide from polymeric matrix with spherical geometry. However, to the best of our knowledge, no general analytical expressions for the concentrations of glucose, oxygen, gluconic acid and hydrogen peroxide for all values of reaction/diffusion parameters have been previously derived. The purpose of the present study was to derive a simple approximate analytical expression for profile concentrations of various species inside the glucose oxidase in chitosan-coated alginate–calcium microspheres (GOX-MS) with steady-state conditions. Furthermore, this model can be used to predict the system performance as well as determining the appropriate combination of material and geometries.

## Mathematical formulation of the problem

Building upon earlier study, Abdekhodaie et al. [5] presented a concise discussion and derivation of the mass transport nonlinear second-order differential equations which gives the concentration profiles of each species within the microsphere membrane. In this section this is summarized briefly below. Figure 1 illustrates the production of hydrogen peroxide as well as the glucose structure loaded in chitosan-alginate microsphere [5, 6]. The reaction of glucose oxidation to produce the gluconic acid and hydrogen peroxide in polymeric microspheres can be written using Eq. (1) as follows:

$$\text{Glucose} + O_2 \xrightarrow{\text{Glucose oxidase}} \text{Gluconic acid} + H_2O_2 \tag{1}$$

Using mass conservation law by neglecting convection, the nonlinear reaction-diffusion equation in spherical coordinate is given by Eq. (2), as follows:

$$\frac{\partial C_i}{\partial t} = \frac{1}{r^2}\frac{\partial}{\partial r}\left(r^2 D_i \frac{\partial C_i}{\partial r}\right) + v_i \mathfrak{R}, \tag{2}$$

where $i$ denotes individual species, e.g. $i = g$ for glucose, $i = OX$ for oxygen, $i = a$ for gluconic acid and $i = h$ for hydrogen peroxide. $v_i$ denotes the stoichiometric coefficients; $C_i$ is the concentration, $D_i$is the diffusion coefficient and $r$ is the length parameter. The overall reaction rate $\mathfrak{R}$ is given by Eq. (3) [7–9]:

$$\mathfrak{R} = \frac{V_{\max} C_g C_{\mathrm{OX}}}{C_{\mathrm{OX}}(K_g + C_g) + C_g K_{\mathrm{OX}}} \tag{3}$$

For steady-state condition Eq. (2) becomes:

$$D_g\left(\frac{\mathrm{d}^2 C_g}{\mathrm{d}r^2} + \frac{2}{r}\frac{\mathrm{d}C_g}{\mathrm{d}r}\right) + \frac{v_g V_{\max} C_g C_{\mathrm{OX}}}{C_{\mathrm{OX}}(K_g + C_g) + C_g K_{\mathrm{OX}}} = 0 \tag{4}$$

$$D_{\mathrm{OX}}\left(\frac{\mathrm{d}^2 C_{\mathrm{OX}}}{\mathrm{d}r^2} + \frac{2}{r}\frac{\mathrm{d}C_{\mathrm{OX}}}{\mathrm{d}r}\right) + \frac{v_{\mathrm{OX}} V_{\max} C_g C_{\mathrm{OX}}}{C_{\mathrm{OX}}(K_g + C_g) + C_g K_{\mathrm{OX}}} = 0 \tag{5}$$

$$D_a\left(\frac{\mathrm{d}^2 C_a}{\mathrm{d}r^2} + \frac{2}{r}\frac{\mathrm{d}C_a}{\mathrm{d}r}\right) + \frac{v_a V_{\max} C_g C_{\mathrm{OX}}}{C_{\mathrm{OX}}(K_g + C_g) + C_g K_{\mathrm{OX}}} = 0 \tag{6}$$

$$D_h\left(\frac{\mathrm{d}^2 C_h}{\mathrm{d}r^2} + \frac{2}{r}\frac{\mathrm{d}C_h}{\mathrm{d}r}\right) + \frac{v_h V_{\max} C_g C_{\mathrm{OX}}}{C_{\mathrm{OX}}(K_g + C_g) + C_g K_{\mathrm{OX}}} = 0, \tag{7}$$

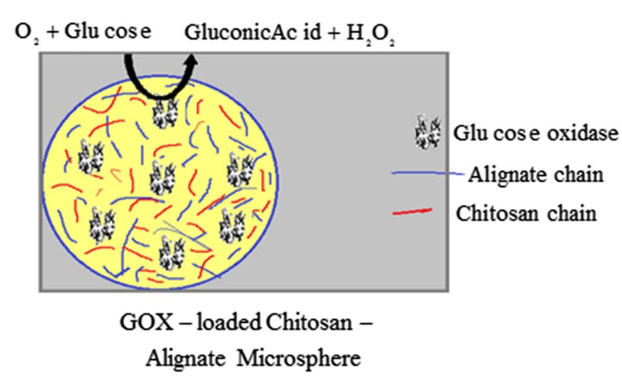


**Fig. 1** Schematic diagram illustrating the structure of a glucose and hydrogen peroxide production in chitosan–aliginate microsphere (Abdekhodaie et al. [5])

**Table 1** Comparison of normalized steady-state concentration of glucose $u$ with simulation results for various values of $\gamma_g$ and for some fixed values of $v_g = -1, \alpha = 13$ and $\beta = 0.4$

| $R$ | Concentration of glucose $u$ | | | | | | | | |
|---|---|---|---|---|---|---|---|---|---|
| | When $\gamma_g = 10$ | | | When $\gamma_g = 20$ | | | When $\gamma_g = 30$ | | |
| | Equation (17) | Simulation | % of error deviation | Equation (17) | Simulation | % of error deviation | Equation (17) | Simulation | % of error deviation |
| 0 | 0.8930 | 0.8939 | 0.10 | 0.8012 | 0.8012 | 0.00 | 0.7219 | 0.7201 | 0.24 |
| 0.2 | 0.8971 | 0.8979 | 0.08 | 0.8086 | 0.8086 | 0.00 | 0.7319 | 0.7302 | 0.23 |
| 0.4 | 0.9096 | 0.9102 | 0.06 | 0.8312 | 0.8311 | 0.01 | 0.7626 | 0.7612 | 0.18 |
| 0.6 | 0.9306 | 0.9311 | 0.05 | 0.8696 | 0.8695 | 0.01 | 0.8155 | 0.8144 | 0.13 |
| 0.8 | 0.9606 | 0.9608 | 0.02 | 0.9253 | 0.9252 | 0.01 | 0.8933 | 0.8928 | 0.05 |
| 1 | 1.0000 | 0.9999 | 0.01 | 1.0000 | 0.9999 | 0.01 | 1.0000 | 0.9999 | 0.01 |
| | Average error % | | 0.143 | Average error % = 0.006 | | | Average error % = 0.140 | | |

**Table 2** Comparison of normalized steady-state concentration of oxygen $v$ with simulation results for various values of $\gamma_{OX}$ and for some fixed values of, $v_g = -1, v_{OX} = -0.5, \gamma_g = 30, \alpha = 13$ and $\beta = 0.4$

| $R$ | Concentration of oxygen $v$ | | | | | | | | |
|---|---|---|---|---|---|---|---|---|---|
| | When $\gamma_{OX} = 20$ | | | When $\gamma_{OX} = 60$ | | | When $\gamma_{OX} = 100$ | | |
| | Equation (18) | Simulation | % of error deviation | Equation (18) | Simulation | % of error deviation | Equation (18) | Simulation | % of error deviation |
| 0 | 0.9073 | 0.9059 | 0.15 | 0.7219 | 0.7187 | 0.44 | 0.5365 | 0.5335 | 0.56 |
| 0.2 | 0.9106 | 0.9093 | 0.14 | 0.7319 | 0.7289 | 0.41 | 0.5532 | 0.5504 | 0.50 |
| 0.4 | 0.9208 | 0.9198 | 0.10 | 0.7626 | 0.7601 | 0.32 | 0.6044 | 0.6020 | 0.39 |
| 0.6 | 0.9385 | 0.9377 | 0.08 | 0.8155 | 0.8137 | 0.22 | 0.6926 | 0.6908 | 0.26 |
| 0.8 | 0.9644 | 0.9640 | 0.04 | 0.8933 | 0.8924 | 0.10 | 0.8222 | 0.8213 | 0.10 |
| 1 | 1.0000 | 0.9999 | 0.01 | 1.0000 | 0.9999 | 0.01 | 1.0000 | 0.9999 | 0.01 |
| | Average error % | | 0.086 | Average error % | | 0.250 | Average error % | | 0.303 |

**Table 3** Comparison of normalized steady-state concentration of gluconic acid $w$ with simulation results for various values of $\gamma_a$ and for some fixed values of, $v_g = -1, v_a = 1, \gamma_g = 30, \alpha = 13$ and $\beta = 0.4$

| $R$ | Concentration of gluconic acid $w$ | | | | | | | | |
|---|---|---|---|---|---|---|---|---|---|
| | When $\gamma_a = 10$ | | | When $\gamma_a = 60$ | | | When $\gamma_a = 120$ | | |
| | Equation (19) | Simulation | % of error deviation | Equation (19) | Simulation | % of error deviation | Equation (19) | Simulation | % of error deviation |
| 0 | 1.0930 | 1.0941 | 0.10 | 1.5560 | 1.5643 | 0.53 | 2.1120 | 2.1287 | 0.78 |
| 0.2 | 1.0893 | 1.0906 | 0.11 | 1.5360 | 1.5437 | 0.49 | 2.0721 | 2.0875 | 0.73 |
| 0.4 | 1.0791 | 1.0802 | 0.10 | 1.4746 | 1.4811 | 0.43 | 1.9492 | 1.9623 | 0.66 |
| 0.6 | 1.0614 | 1.0622 | 0.07 | 1.3688 | 1.3734 | 0.33 | 1.7376 | 1.7470 | 0.53 |
| 0.8 | 1.0355 | 1.0359 | 0.03 | 1.2132 | 1.2155 | 0.18 | 1.4265 | 1.4312 | 0.32 |
| 1 | 1.0000 | 1.0000 | 0.00 | 1.0000 | 0.9999 | 0.01 | 1.0000 | 1.0000 | 0.00 |
| | Average error % | | 0.068 | Average error % | | 0.328 | Average error % | | 0.503 |

where $D_g$, $D_{OX}$, $D_a$ and $D_h$ are the diffusion coefficients of glucose, oxygen, gluconic acid and hydrogen peroxide, respectively. Since the coefficient is also dependent upon the material of the microspheres, generally, here we can assume that all the diffusion coefficients are different $C_g$, $C_{OX}$, $C_a$ and $C_h$ from the corresponding concentrations, where $r$ is the spatial coordinate; and $V_{max}$ is the maximal reaction velocity that is proportional to the concentration of enzyme ($C_{enz}$) in the microspheres. $K_g$ and $K_{OX}$ denote the Michaelis–Menton constant and catalytic rate constant for glucose and glucose oxidase, respectively. The boundary conditions are given by Eqs. (8) and 9:

**Table 4** Comparison of normalized steady-state concentration of hydrogen peroxide $H$ with simulation results for various values of $\gamma_h$ and for some fixed values of, $v_g = -1, v_h = 1, \gamma_g = 30, \alpha = 13$ and $\beta = 0.4$

| $R$ | Concentration of hydrogen peroxide $H$ | | | | | | | | |
|---|---|---|---|---|---|---|---|---|---|
| | When $\gamma_a = 12$ | | | When $\gamma_a = 45$ | | | When $\gamma_a = 85$ | | |
| | Equation (20) | Simulation | % of error deviation | Equation (20) | Simulation | % of error deviation | Equation (20) | Simulation | % of error deviation |
| 0 | 1.1110 | 1.1129 | 0.17 | 1.4170 | 1.4233 | 0.44 | 1.7880 | 1.7995 | 0.63 |
| 0.2 | 1.1072 | 1.1087 | 0.13 | 1.4020 | 1.4078 | 0.41 | 1.7594 | 1.7703 | 0.61 |
| 0.4 | 1.0949 | 1.0962 | 0.11 | 1.3559 | 1.3609 | 0.36 | 1.6724 | 1.6816 | 0.54 |
| 0.6 | 1.0737 | 1.0747 | 0.09 | 1.2766 | 1.2801 | 0.30 | 1.5225 | 1.5291 | 0.43 |
| 0.8 | 1.0426 | 1.0431 | 0.04 | 1.1599 | 1.1617 | 0.15 | 1.3021 | 1.3054 | 0.25 |
| 1 | 1.0000 | 1.0000 | 0.00 | 1.0000 | 1.0000 | 0.00 | 1.0000 | 1.0000 | 0.00 |
| | Average error % | | 0.090 | Average error % | | 0.276 | Average error % | | 0.410 |

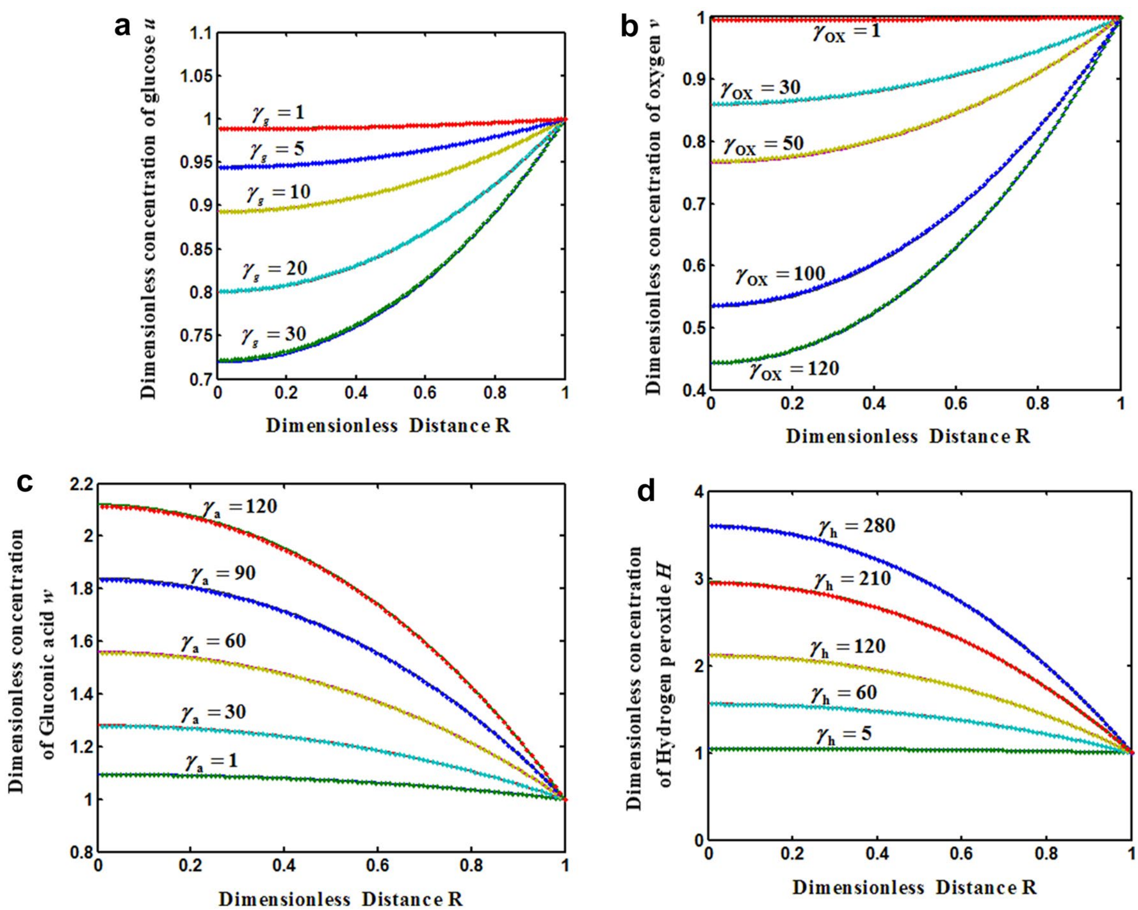


**Fig. 2** Comparison of analytical expression of concentration of glucose Eq. (17), oxygen Eq. (18), gluconic acid Eq. (19) and hydrogen peroxide Eq. (20) with simulation results for various parameters. **a** $\alpha = 13, \beta = 0.4$ and $v_g = -1$, **b** $\alpha = 13, \beta = 0.4, \gamma_g = 30, v_g = -1$ and $v_{OX} = -0.5$, **c** $\alpha = 13, \beta = 0.4, \gamma_g = 30, v_g = -1$ and $v_a = 1$, **d** $\alpha = 13, \beta = 0.4, \gamma_g = 30, v_g = -1$ and $v_h = 1$ dotted lines represent the analytical solution and solid lines the numerical solution

$$r = 0, \frac{dC_g}{\partial r} = 0, \frac{dC_{ox}}{\partial r} = 0, \frac{dC_a}{\partial r} = 0, \frac{dC_h}{\partial r} = 0 \tag{8}$$

$$r = S, C_g = C_g^*, C_{OX} = C_{OX}^*, C_a = C_a^*, C_{h'} = C_h^*, \tag{9}$$

where $S$ is radius of the microsphere, $r=0$ is the center of the microsphere and $C_{OX}^*$ and $C_g^*$ are the concentrations of oxygen and glucose in the external solution, respectively. Using the following dimensionless variables

$$u = \frac{C_g}{C_g^*}; v = \frac{C_{OX}}{C_{OX}^*}; w = \frac{C_a}{C_a^*}; H = \frac{C_h}{C_h^*}; R = \frac{r}{S}; \tag{10}$$

$$\gamma_g = \frac{V_{max}S^2}{D_g C_g^*}; \gamma_{OX} = \frac{V_{max}S^2}{D_{OX}C_{OX}^*}; \gamma_a = \frac{V_{max}S^2}{D_a C_a^*};$$
$$\gamma_h = \frac{V_{max}S^2}{D_h C_h^*}; \alpha = \frac{K_g}{C_g^*}; \beta = \frac{K_{OX}}{C_{OX}^*} \tag{11}$$

Equations (4)–(7) can be written in the following dimensionless form:

$$\frac{d^2u}{dR^2} + \frac{2}{R}\frac{du}{dR} + v_g\gamma_g uv(\alpha v + uv + \beta u)^{-1} = 0 \tag{12}$$

$$\frac{d^2v}{dR^2} + \frac{2}{R}\frac{dv}{dR} + v_{OX}\gamma_{OX} uv(\alpha v + uv + \beta u)^{-1} = 0 \tag{13}$$

$$\frac{d^2w}{dR^2} + \frac{2}{R}\frac{dw}{dR} + v_a\gamma_a uv(\alpha v + uv + \beta u)^{-1} = 0 \tag{14}$$

$$\frac{d^2H}{dR^2} + \frac{2}{R}\frac{dH}{dR} + v_h\gamma_h uv(\alpha v + uv + \beta u)^{-1} = 0. \tag{15}$$

Here *u, v, w* and *H* are the dimensionless concentrations of glucose, oxygen, gluconic acid and hydrogen peroxide

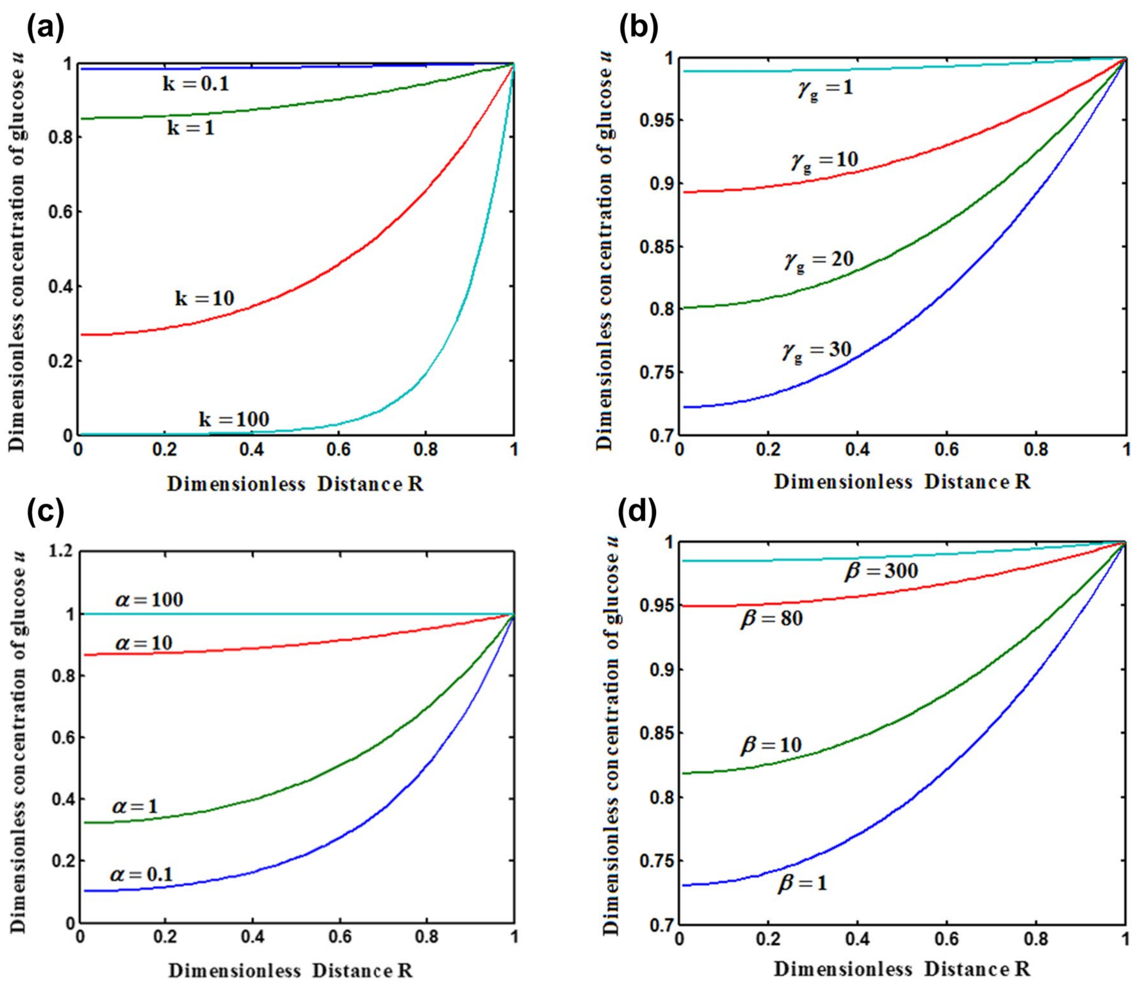


**Fig. 3** Plot of concentration profiles of glucose $u(R)$ versus dimensionless distance $R$ calculated using Eq. (17) for values of: **a** Thiele modulus $k$, **b** $\alpha = 13, \beta = 0.4, v_g = -1$ and various values of the Thiele modulus $\gamma_g$ **c** $\beta = 0.4, v_g = -1, \gamma_g = 30$ and various values of parameter $\alpha$. **d** $\alpha = 13, v_g = -1, \gamma_g = 30$ and various values of parameter $\beta$

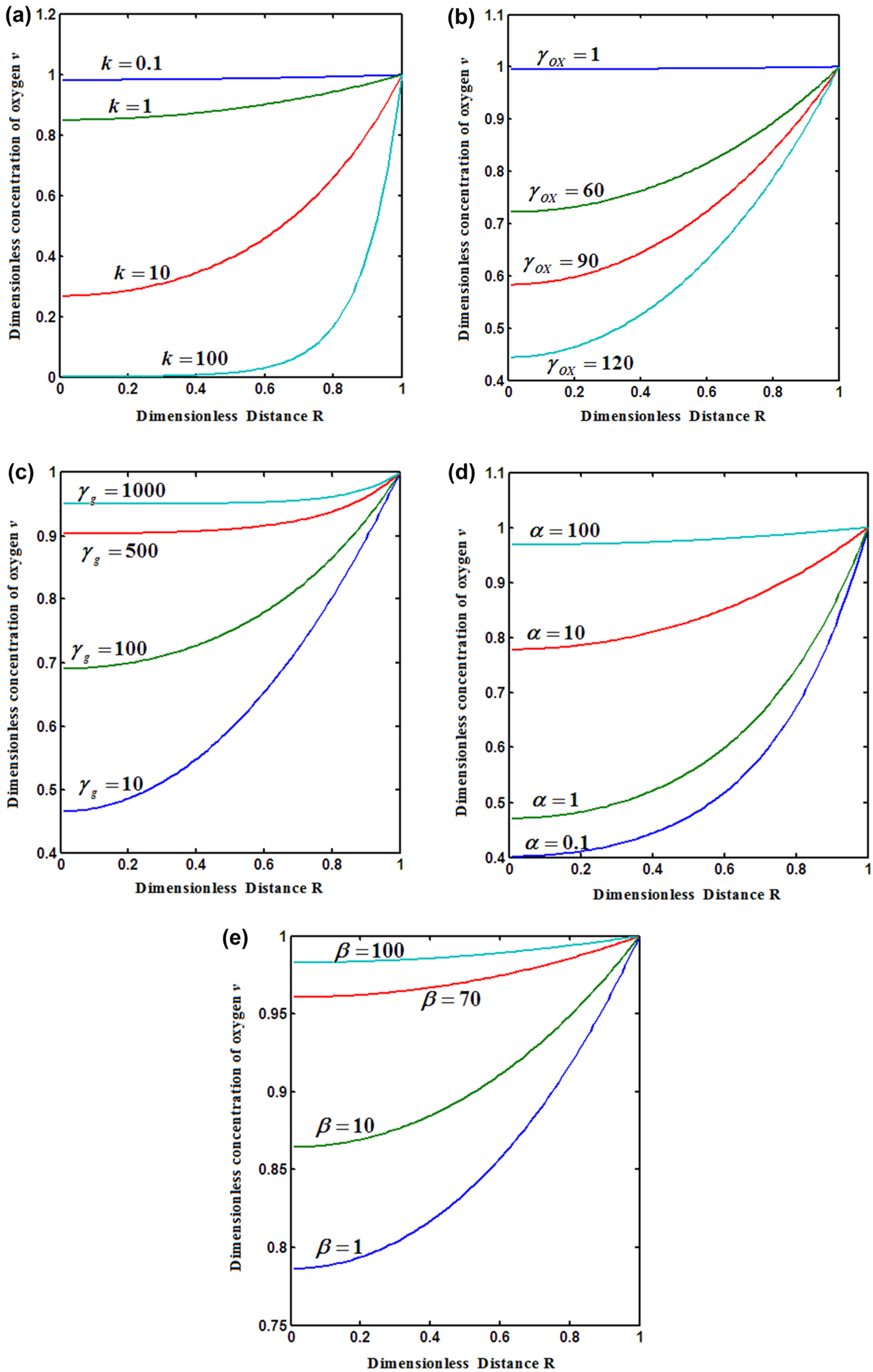
(a)
$k = 0.1$
$k = 1$
$k = 10$
$k = 100$
Dimensionless concentration of oxygen $v$
Dimensionless Distance R
(b)
$\gamma_{OX} = 1$
$\gamma_{OX} = 60$
$\gamma_{OX} = 90$
$\gamma_{OX} = 120$
Dimensionless concentration of oxygen $v$
Dimensionless Distance R
(c)
$\gamma_g = 1000$
$\gamma_g = 500$
$\gamma_g = 100$
$\gamma_g = 10$
Dimensionless concentration of oxygen $v$
Dimensionless Distance R
(d)
$\alpha = 100$
$\alpha = 10$
$\alpha = 1$
$\alpha = 0.1$
Dimensionless concentration of oxygen $v$
Dimensionless Distance R
(e)
$\beta = 100$
$\beta = 70$
$\beta = 10$
$\beta = 1$
Dimensionless concentration of oxygen $v$
Dimensionless Distance R

◂**Fig. 4** Plot of concentration profiles of oxygen $v(R)$ versus dimensionless radius of microsphere $R$ calculated using Eq. (18) for the values of: **a** $v_g = -1, \gamma_g = 30, v_{OX} = -0.5, \gamma_{OX} = 60$ for various values of $k$. **b** $v_g = -1, \gamma_g = 30, v_{\mathrm{OX}} = -0.5, \alpha = 13, \beta = 0.4$ various values of Thiele modulus $\gamma_{\mathrm{OX}}$, **c** $v_g = -1, v_{\mathrm{OX}} = -0.5, \alpha = 13, \beta = 0.4, \gamma_{\mathrm{OX}} = 100$ various values of $\gamma_g$. **d** $v_g = -1, \gamma_g = 30, v_{\mathrm{OX}} = -0.5, \gamma_{\mathrm{OX}} = 40, \beta = 0.4$ and for various values of parameter $\alpha$. **e** $v_g = -1, \gamma_g = 30, v_{\mathrm{OX}} = -0.5, \gamma_{\mathrm{OX}} = 40, \alpha = 10$ and for various values of parameter $\beta$

respectively, and $\gamma_g$ and $\gamma$ are the corresponding Thiele modulus. $\alpha$ and $\beta$ are the dimensionless rate constants. The corresponding boundary conditions [Eqs. (8), (9)] becomes:

$$R = 0,\ \frac{\mathrm{d}u}{\mathrm{d}R} = 0,\ \frac{\mathrm{d}v}{\mathrm{d}R} = 0,\ \frac{\mathrm{d}w}{\mathrm{d}R} = 0,\ \frac{\mathrm{d}H}{\mathrm{d}R} = 0 \tag{16}$$

$$R = 1,\ u = 1,\ v = 1,\ w = 1,\ H = 1. \tag{17}$$

## Approximate analytical expression for the concentration of glucose, oxygen, gluconic acid and hydrogen peroxide using HPM

Nonlinear partial differential equations have been employed to model different problems encountered in engineering and natural sciences disciplines. Over the years, nonlinear science, in particular, analytical techniques for nonlinear science, has attracted a great attention from physicists and engineers. However, like other nonlinear analytical techniques, the existing perturbation methods have their own limitations [10, 11]. These facts have motivated to suggest alternative techniques, such as variational iteration [12, 13] as well as Adomain decomposition [14–17], exp function [18] method and homotopy perturbation method (HPM). Lately, Rajendran and Anitha [19] solved nonlinear problem in amperometric enzyme electrodes using a new approach of homotopy perturbation method. More recently, Zhen-Jiang et al. [20] employed the homotopy perturbation method and Laplace transformation to find the exact solutions of some non-linear PDE. This method is very easy to implement due to the flexibility associated in choosing its initial approximation. Adamu and Ogenyi [21] successfully solved duffing oscillator problem using a new modification of the homotopy parameter. This new technique is proved to be powerful and efficient.

The basic principle of this method is described in ESM Appendix A. We have obtained the analytical expressions of the concentrations of glucose, oxygen, gluconic acid and hydrogen peroxide by solving the nonlinear Eqs. (12)–(15) using the new approach of homotopy perturbation method [22, 23] as follows (ESM Appendix B and C):

$$u(R) \approx \frac{\sin\ h\left(\sqrt{K}R\right)}{R\sin\ h\left(\sqrt{K}\right)} \tag{18}$$

$$v(R) \approx 1 + \frac{v_{\mathrm{OX}}\gamma_{\mathrm{OX}}}{v_g\gamma_g}(u(R) - 1) \tag{19}$$

$$w(R) \approx 1 + \frac{v_a\gamma_a}{v_g\gamma_g}\ (\,u(R) - 1\,) \tag{20}$$

$$H(R) \approx 1 + \frac{v_h\gamma_h}{v_g\gamma_g}\ (\,u(R) - 1\,) \tag{21}$$

where $k = v_g\gamma_g/(\alpha + 1 + \beta)$.

Equations (18)–(21) represent the new analytical expression of concentration of glucose, oxygen, gluconic acid and hydrogen peroxide. Detailed derivations of the dimensionless concentration of glucose, oxygen, gluconic acid and hydrogen peroxide are described in Appendix B, C.

## Numerical simulation

The nonlinear reaction diffusion is given by Eqs. (12)–(15) for the corresponding boundary conditions. [Eq. (15) and Eq. (16)] are also solved numerically by using Scilab program (ESM Appendix D) in which the Stoichiometric coefficients $v_i$ are given by:$v_g = -1$, $v_{OX} = -0.5$, $v_a = 1, v_h = 1$, respectively [5, 6, 8]. The numerical solutions are compared with our analytical results in Tables 1, 2, 3 and 4 and in Fig. 2. The maximum average error between our analytical results and the simulation results for the concentration of glucose, oxygen, gluconic acid and hydrogen peroxide are 0.09, 0.21, 0.29 and 0.25%, respectively.

## Relation between the concentration of glucose, oxygen, gluconic acid and hydrogen peroxide

Equation (22) represents the relation between glucose, oxygen, gluconic acid and hydrogen peroxide concentration for all values of kinetics parameters

$$\begin{aligned} &u(R)\left(\frac{v_{\mathrm{OX}}\gamma_{\mathrm{OX}}}{v_g\gamma_g} + \frac{v_a\gamma_a}{v_g\gamma_g} + \frac{v_h\gamma_h}{v_g\gamma_g}\right) - v(R) - w(R) - H(R) \\ &\quad = \frac{v_{\mathrm{OX}}\gamma_{\mathrm{OX}}}{v_g\gamma_g} + \frac{v_a\gamma_a}{v_g\gamma_g} + \frac{v_h\gamma_h}{v_g\gamma_g} - 3. \end{aligned} \tag{22}$$

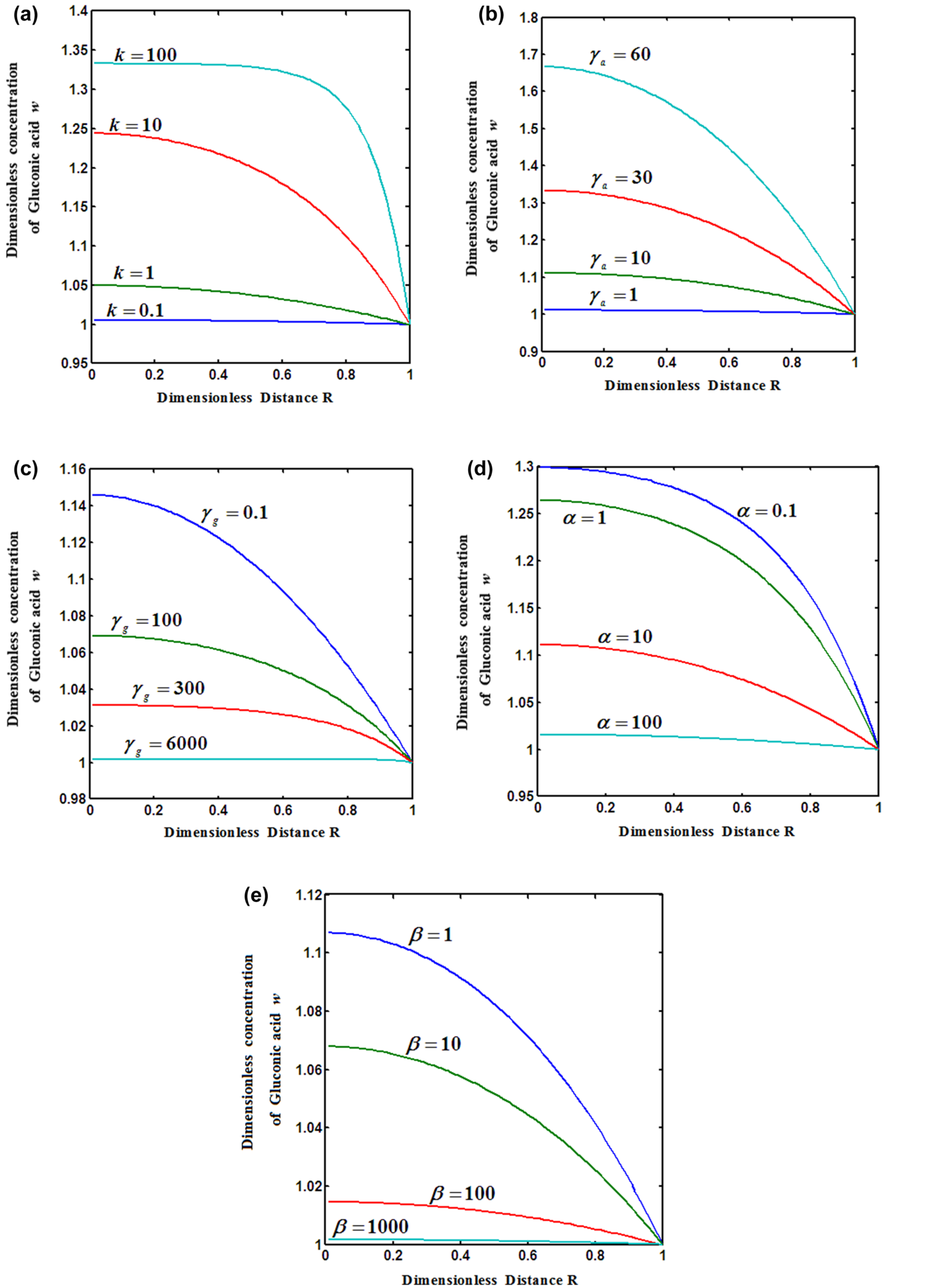
(a)
Dimensionless concentration of Gluconic acid w
Dimensionless Distance R
k = 100
k = 10
k = 1
k = 0.1
(b)
γa = 60
γa = 30
γa = 10
γa = 1
(c)
γg = 0.1
γg = 100
γg = 300
γg = 6000
(d)
α = 0.1
α = 1
α = 10
α = 100
(e)
β = 1
β = 10
β = 100
β = 1000

◂**Fig. 5** Plot of concentration profiles of gluconic acid $w(R)$ versus dimensionless distance $R$ calculated using Eq. (19) for values of: **a** $\gamma_g = 30, v_g = -1, \gamma_a = 10, v_a = 1$ and various values $k$. **b** $v_g = -1, \gamma_g = 30,\ v_a = 1, \alpha = 10, \beta = 0.4$ for various values of $\gamma_a$. **c** $v_g = -1,\ v_a = 1, \alpha = 10, \beta = 0.4, \gamma_a = 10$ and various values of $\gamma_g$. **d** $v_g = -1, \gamma_g = 30, v_a = 1, \gamma_a = 10, \beta = 0.4$ and various values of parameter $\alpha$. **e** $v_g = -1, \gamma_g = 30, v_a = 1, \alpha = 10, \gamma_a = 10$ and various values of parameter $\beta$

## Determination flux of hydrogen peroxide

The flux of hydrogen peroxide from the surface is defined by Fick's first law:

$$(J_h) = -D\left(\frac{\partial C_h}{\partial r}\right)_{r=S} = -D\left(\frac{C_h^*}{S}\frac{\partial H}{\partial R}\right)_{R=1} . \tag{23}$$

Using Eqs. (21) and (23) the flux becomes:

$$J_h = \frac{-D \cdot C_h^*}{S}\left(\sqrt{k}\coth\sqrt{k} - 1\right). \tag{24}$$

Equation (23) represents the new simple analytical expression of flux of hydrogen peroxide.

## Determination of pH profile inside the microspheres

The pH in the presence of gluconic acid is determined by the concentration of buffer ions and gluconic acid in the microsphere.

$$pH_2 = pK + \log\left\{\frac{10^{pH_1-pK} - \left(\frac{C_a}{[\text{buffer}]}\right)\left(1 + 10^{pH_1-pK}\right)}{1 + \left(\frac{C_a}{[\text{buffer}]}\right)\left(1 + 10^{pH_1-pK}\right)}\right\} \tag{25}$$

Using the Eq. (20), we obtain the pH in the presence of gluconic acid as follows:

$$\exp(pH_2 - pK) = \left\{\frac{10^{pH_1-pK} - \left(\left(1 + \frac{v_a\gamma_a}{v_g\gamma_g}\left(\frac{\sin\ h\left(\sqrt{k}R\right)}{R\sin\ h\left(\sqrt{k}\right)} - 1\right)\right)\frac{C_a^*}{[\text{buffer}]}\right)\left(1 + 10^{pH_1-pK}\right)}{1 + \left(\left(1 + \frac{v_a\gamma_a}{v_g\gamma_g}\left(\frac{\sinh\left(\sqrt{k}R\right)}{R\sinh\left(\sqrt{k}\right)} - 1\right)\right)\frac{C_a^*}{[\text{buffer}]}\right)\left(1 + 10^{pH_1-pK}\right)}\right\}. \tag{26}$$

## Results and discussion

Equations (18)–(21) represent the new approximate analytical expression for the concentrations of glucose, oxygen, gluconic acid and hydrogen peroxide for all the parameter values. From Fig. 2a and b, it is observed that the concentrations of glucose and oxygen are depleted at the center of the microsphere ($R = 0$) as they are consumed by the enzyme reaction. The slope decreases in the presence of glucose and oxygen increase with the increase in Thiele modulus or radius of the microsphere. Since glucose and oxygen together form gluconic acid at the center of the microsphere, gluconic acid's concentration increases with the increase in the Thiele modulus or enzyme concentration.

### Influence of radius of microsphere over the concentration of glucose ($u$)

The radius of chitosan alginate microsphere plays a crucial role as the dynamic process involving diffusion of reactants and product is coupled with an enzymatic reaction inside the microsphere. The concentration of glucose depends on the permeability of reactants and products through the membrane. From Fig. 3 it is inferred that when the Thiele modulus $\gamma_g$ or $\gamma$ which depends on the radius of microsphere or enzyme concentration is increased, the concentration of glucose ($u$) decreases. The thicker the radius of microsphere, the lower the concentration of glucose. The concentration of glucose drops towards to 0 when the value of parameter $k \geqslant 100$ and $\alpha < 0.1$.

### Influence of the maximal reaction velocity ($V_{max}$) on the concentration of oxygen($v$)

Increasing the substrate (glucose) concentration indefinitely does not increase the rate of an enzyme-catalyzed reaction beyond a certain point. In order to achieve that particular point, there is need to be enough substrate molecules to completely fill (saturate) the enzyme's active sites. How quickly the enzyme is catalyzed by the reaction is indicated by $V_{\max}$.

In this enzymatic reaction diffusion process, the maximal reaction velocity $V_{\max}$ is proportional to the concentration of the enzyme in the microsphere and the overall kinetics are determined by the maximal reaction rate. From Figs. 2, 3 and 4, it is clear that as the reaction diffusion parameters $\gamma_g$ or $\gamma_{\text{OX}}$ increase, or the concentration of $\gamma_a, \gamma_h$ decreases gradually; it becomes zero for higher values of the reaction velocity.

### Influence of concentration of glucose in the external solution over the concentration of gluconic acid ($w$)

The concentration of gluconic acid and hydrogen peroxide is determined by the concentration of glucose, the permeability of reactants through the membrane and the enzymatic reaction rate. From Figs. 5 and 6, it is evident that the concentration of gluconic acid and hydrogen peroxide keeps increasing by decreasing the Thiele modulus ($\gamma_g$) which depends on the initial concentration of glucose $\left(C_g{}^*\right)$.

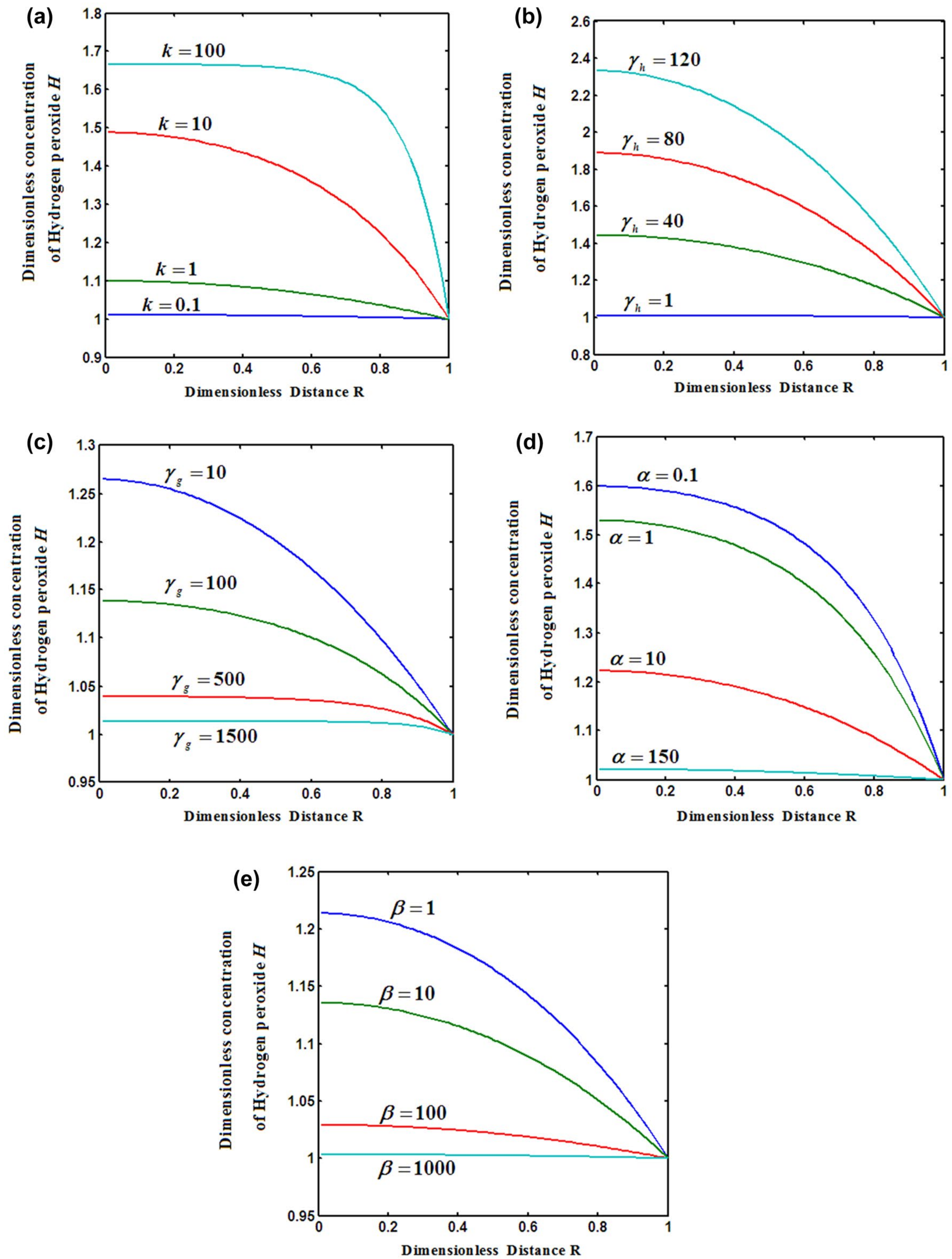


**Fig. 6** Plot of concentration profiles of hydrogen peroxide $H(R)$ versus dimensionless distance $R$ calculated using Eq. (20) for the values of: **a** $\gamma_g = 30$, $v_g = -1, \gamma_h = 20, v_h = 1$ and various values $k$. **b** $v_g = -1, \gamma_g = 30$, $v_h = 1, \alpha = 10, \beta = 0.4$ for various values of $\gamma_h$. **c** $v_g = -1$, $v_h = 1, \alpha = 10, \beta = 0.4, \gamma_h = 20$ and various values of $\gamma_g$, **d** $v_g = -1, \gamma_g = 30$, $v_h = 1, \gamma_h = 20, \beta = 0.4$ and various values of parameter $\alpha$. **e** $v_g = -1, \gamma_g = 30$, $v_h = 1, \alpha = 10, \gamma_h = 20$ and various values of parameter $\beta$

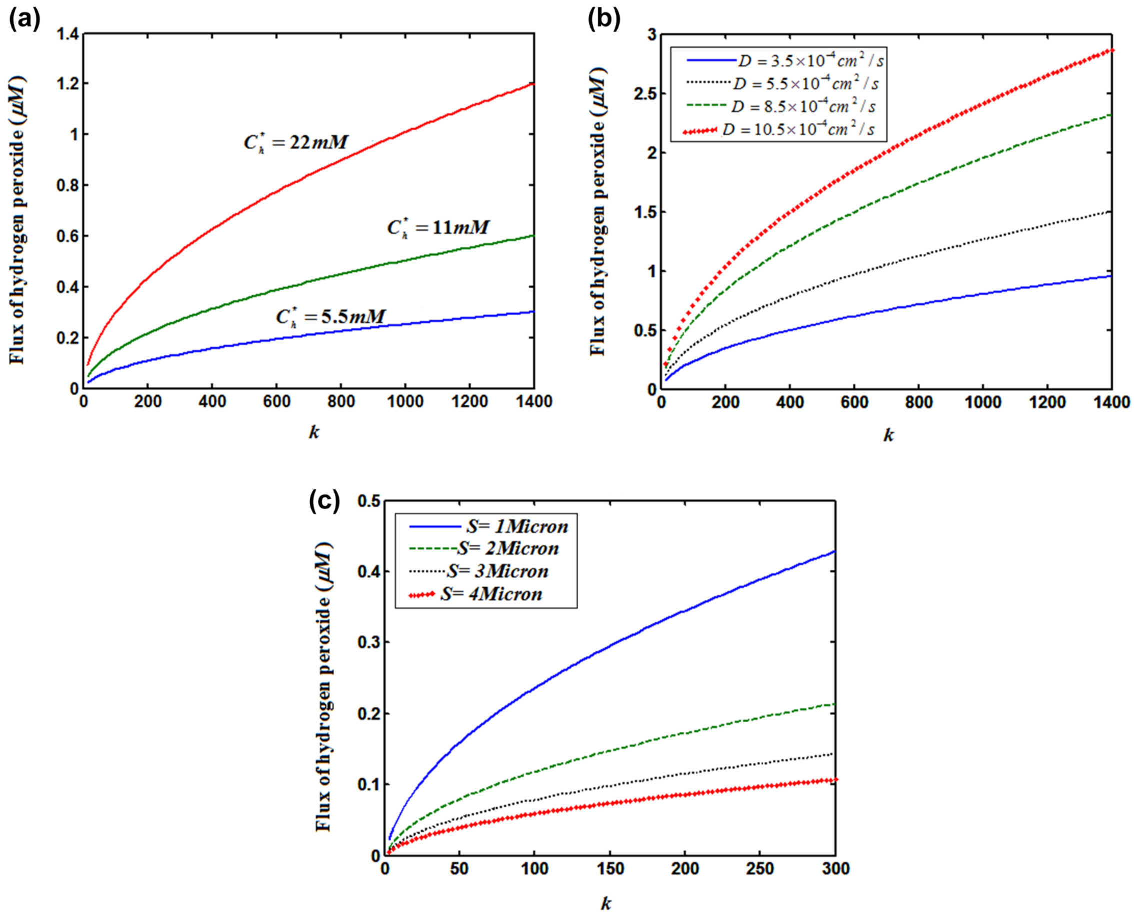


**Fig. 7** Flux of hydrogen peroxide versus dimensionless parameter $k$ for various values of: **a** $D = 1.5 \times 10^{-5}$ cm$^2$/s, S = $1 \times 10^{-5}$cm, **b** $D = 3.5 \times 10^{-5}$cm$^2$/s, $C_h^* = 0.075 \times 10^{-3}$mol/cm$^3$, S = $1 \times 10^{-4}$cm, **c** $D = 3.5 \times 10^{-5}$cm$^2$/s, $C_g^* = 0.075 \times 10^{-3}$mol/cm$^3$

## Influence of various parameters on the flux of the hydrogen peroxide

Figure 7shows the flux of hydrogen peroxide versus $k$ for various parameters $C_g^*, D_s$ and $S$. From this Fig. 7 it is observed that the glucose concentration in the external solution increases the hydrogen peroxide release rate. This is due to an internal pH decrease and less hydrogen peroxide permeability.

The dimensionless parameter $k$ depends upon Thiele moduli and Michaelis constants. Thiele modules are directly proportional to maximum reaction rate and radius of the microsphere, whereas it is inversely proportional to diffusion coefficients and concentration of glucose and oxygen in the external solution.

Figure 8 represents $\exp(pH_2 - pK)$ versus $pH_1 - pK$. From this figure it is observed that $\exp(pH_2 - pK)$ uniformly increases when $C_a$/[buffer $\geqslant 0.5$]. From the figure it is inferred that $C_a$/[buffer] approaches zero when the pH of a buffer in the presence of gluconic acid is equal to the pH in the absence of gluconic acid.

## Influence of parameter *k* on the concentration of glucose, oxygen, gluconic acid and hydrogen peroxide at the center of the microsphere

From the Eqs. (18–21) we can obtain the concentration of glucose, oxygen, gluconic acid and hydrogen peroxide which is given in the Table 5. Figure 9 contains plots of glucose, oxygen, gluconic acid and hydrogen peroxide versus dimensionless parameter $k$. From Figs. 9 and 10 is inferred that the concentration of glucose and oxygen decreases as the parameter $k$ increases. In addition, the concentration of gluconic acid and hydrogen peroxide also increases when the parameter $k$ increases. This is due to an increment in the constant balance between diffusional supply and enzymatic consumption of oxygen and glucose.

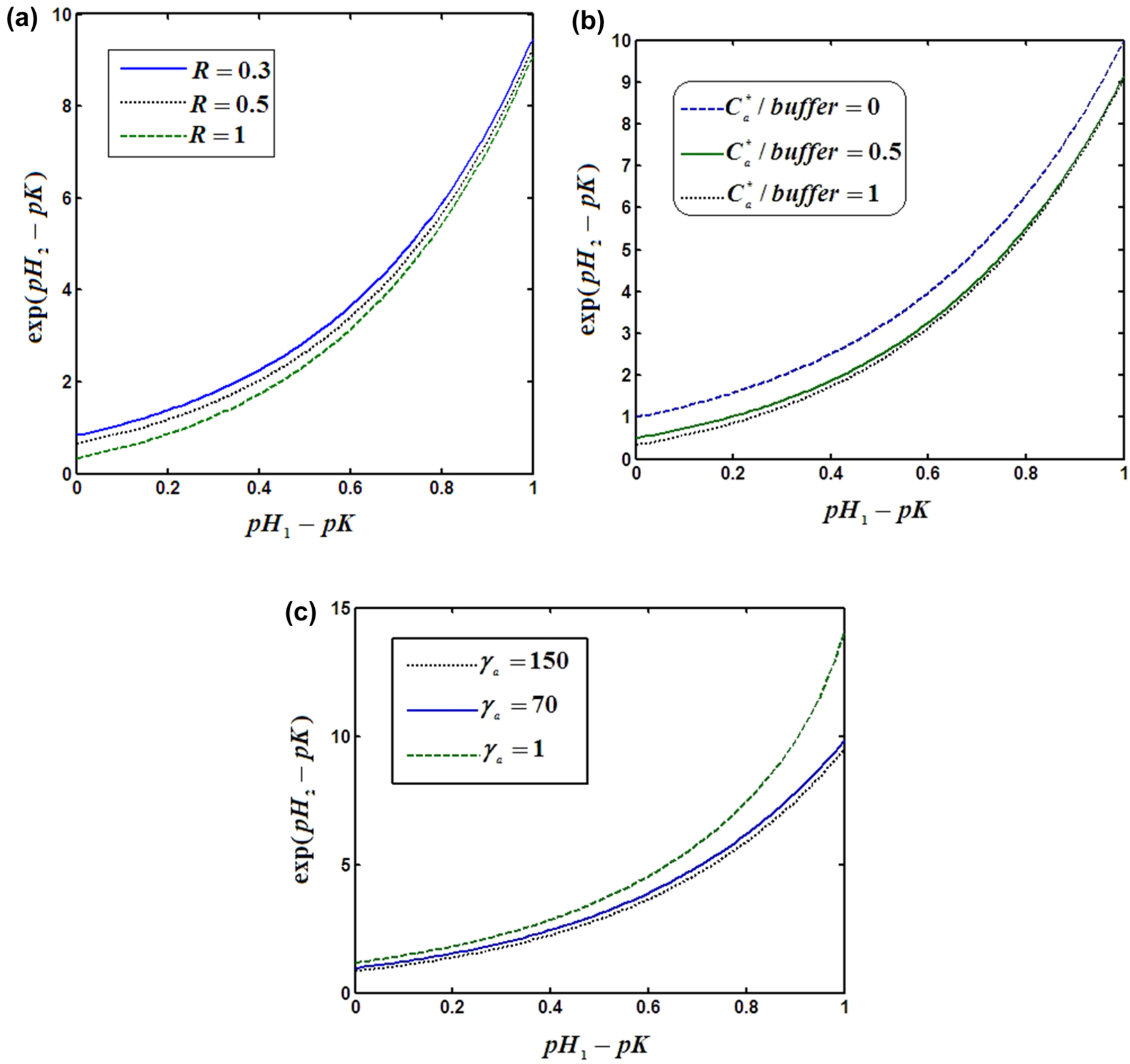


**Fig. 8** Plot of $\exp(pH_2 - pK)$ versus $pH_1 - pK$ when the other parameters are **a** $v_g = -1, \gamma_g = 20, v_a = 1, \gamma_a = 70, \alpha = 13,\ \beta = 0.01$ and $\frac{c_a^*}{[\text{buffer}]} = 1$, **b** $v_g = -1, \gamma_g = 30, v_a = 1, \gamma_a = 60, \alpha = 1,\ \beta = 10,$ and $R = 1$, **c** $v_g = -1, \gamma_g = 10, v_a = 1, \gamma_a = 150,\ \alpha = 1,\ \beta = 13,\ R = 0.2$ and $\frac{c_a^*}{[\text{buffer}]} = 0.1$

**Table 5** Concentration of glucose, oxygen, gluconic acid and hydrogen peroxide at the center of the microsphere

| Concentration | Steady-state expression |
|---|---|
| Glucose | $u(R=0) = \frac{\sqrt{k}}{\sinh\sqrt{k}}$ |
| Oxygen | $v(R=0) = 1 + \frac{v_{\mathrm{ox}}\gamma_{\mathrm{ox}}}{v_g\gamma_g}\left(\frac{\sqrt{k}}{\sinh\sqrt{k}} - 1\right)$ |
| Gluconic acid | $w(R=0) = 1 + \frac{v_a\gamma_a}{v_g\gamma_g}\left(\frac{\sqrt{k}}{\sinh\sqrt{k}} - 1\right)$ |
| Hydrogen peroxide | $H(R=0) = 1 + \frac{v_h\gamma_h}{v_g\gamma_g}\left(\frac{\sqrt{k}}{\sinh\sqrt{k}} - 1\right)$ |

## Differential sensitivity analysis of parameters

Model parameters exerting the most influence on model results are identified through a differential sensitivity analysis [24]. Sensitivity analysis of the parameters is given in Fig. 9a–d in the supplementary material. From the analysis it is inferred that the reaction and diffusion parameters $\alpha, \beta$ have more impact in the concentrations of glucose, oxygen and gluconic acid when it is varied. In contrast the parameter $\gamma_g, \gamma$ accounts for only small changes in the concentrations of glucose, oxygen and gluconic acid.

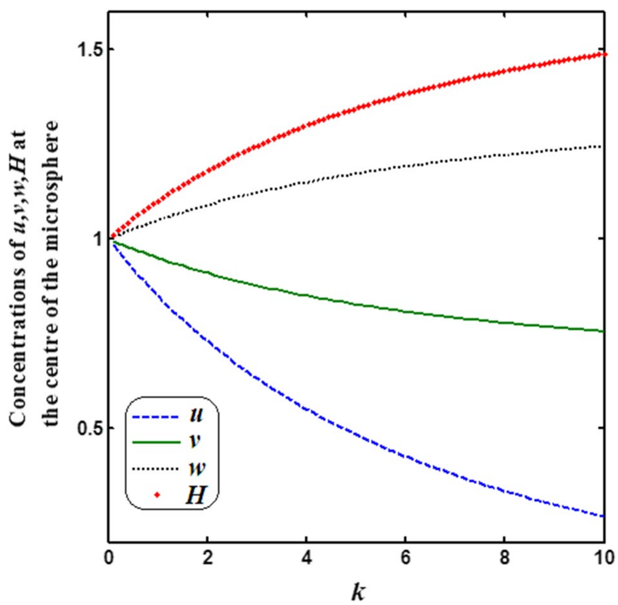


**Fig. 9** Plot of concentration profiles of glucose, oxygen, gluconic acid and hydrogen peroxide at the center of microsphere versus k for steady-state condition. The values of parameters are: $v_g = -1$, $v_{OX} = -0.5, v_a = 1, v_h = 1, \gamma_g = 30$, $\gamma_{OX} = 20$, $\gamma_a = 10$, $\gamma_h = 20$

## Conclusions

A mathematical model of glucose oxidase-loaded microsphere has been successfully discussed. The model illustrated the $H_2O_2$ kinetics production from the GOX-loaded spherical polymeric matrix. A system of nonlinear reaction diffusion equations for steady-state conditions depicted in this model has been solved analytically. From the obtained analytical results, glucose, gluconic and oxygen values for diffusivity and concentrations have been effectively forecasted. The accuracy of the presented methodology was commendably demonstrated by comparing the analytical with the numerical results. The influence of various parameters (glucose concentration in the external solution, particle size, enzyme loading, Michaelis constant, etc) on the concentration of gluconic acid and hydrogen peroxide release has been efficiently discussed. Furthermore, this theoretical model can be successfully applied to optimize the performance of hydrogen peroxide delivery systems as well as to obtain the parameters required for improving the design of the system.

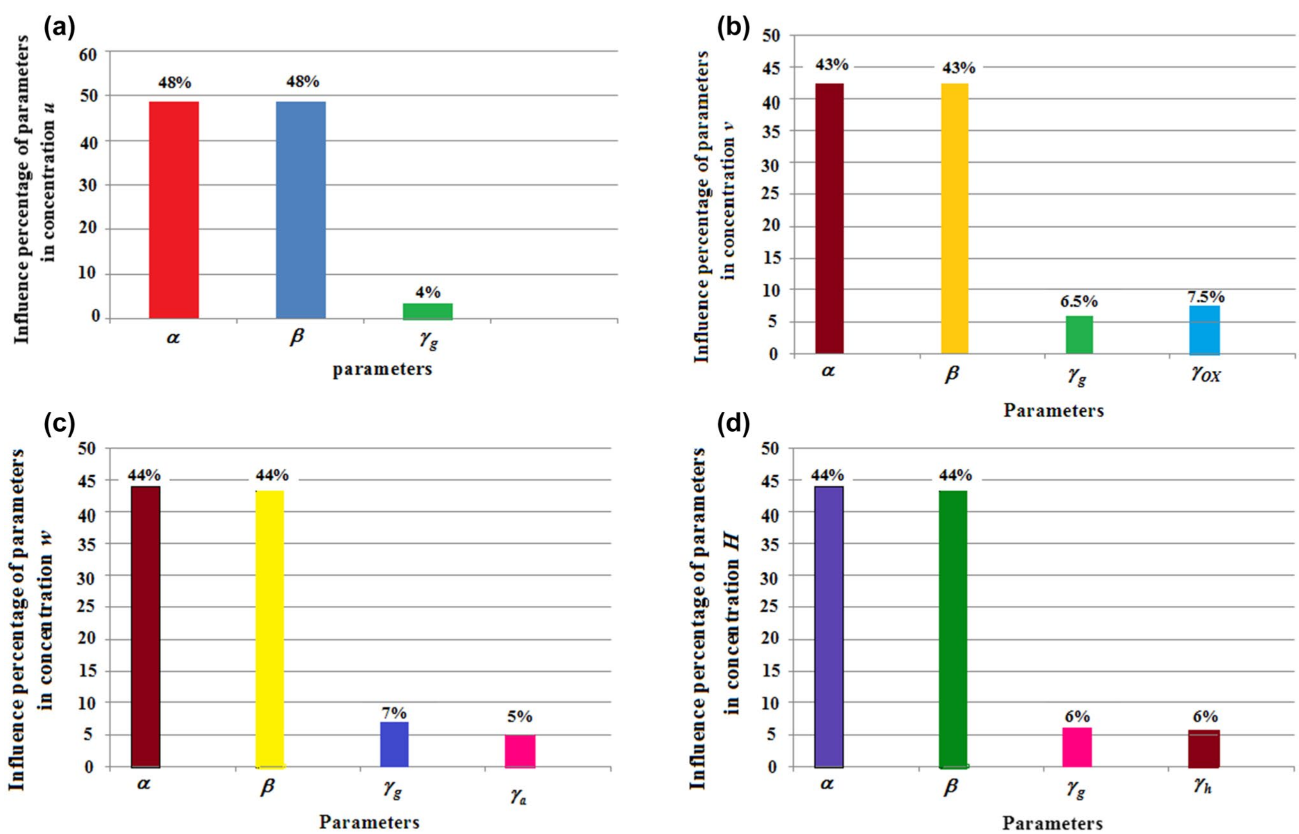


**Fig. 10** Influence percentage of parameters in different concentrations: **a** μ; **b** ν; **c** w and **d** H

## Compliance with ethical standards

**Conflict of interest** There are no conflicts of interests.

## References


1. Szatrowski TP, Nathan CF (1991) Production of large amounts of hydrogen peroxide by human tumor cells. Cancer Res 51:794–798
2. Abdekhodaie MJ, Wu XY (2009) Modeling of a glucose sensitive composite membrane for closed loop insulin delivery. J Membr Sci 335:21–31
3. Albin G, Horbett TA, Ratner BD (1990) Glucose sensitive membranes for controlled deliver of insulin. In: Kost J (ed) pulsed and self-regulated drug delivery. CRC Press, Boca Raton. F, pp 159–185
4. Rajendran L, Bieniasz LK (2012) Analytical expressions for the steady-state concentrations of glucose, oxygen and gluconic acid in a composite membrane for closed-loop insulin delivery. J Membrane Biol 246:121–129
5. Abdekhodaie MJ, Cheng JI, Wu XY (2015) Effect of formulation factors on the bioactivity of glucose oxidase encapsulated chitosan-alginate microspheres: In vitro investigation and mathematical model prediction. Chem Eng Sci 125:4–12
6. Abdekhodaie MJ, Wu XY (2005) Modeling of a cationic glucose sensitive membrane with consideration of oxygen limitation. J Membr Sci 245:119–127
7. Gough DA, Lusisano JY, Tse PHS (1985) Two-dimensional enzyme electrode sensor for glucose. Anal Chem 57:2351–2357
8. Klumb LA, Horbett TA (1992) Design of insulin delivery devices based on glucose sensitive membranes. J Control Release 18:59–80
9. Trachootham D, Alexandre J, Huang P (2009) Targeting cancer cells by ROS-mediated mechanisms: a radical therapeutic approach? Nat RevDrug Discov 8:579–891
10. He JH (2006) Homotopy perturbation method for solving boundary value problems. Phy Lett A 350:87–88
11. He JH (2004) Comparison of homotopy perturbation method and homotopy analysis method. Appl Math Comput 156:527–539
12. He JH Hong Wu Xu (2006) Construction of solitary solution and compact on-like solution by variational iteration method. Chaos Solitons Fractols 29:108–113
13. He JH,Wu XH (2007) Variational iteration method: new development and applications. Comput Math Appl 54:881–894
14. Adomian G, Witten M (1994) Computation of solutions to the generalized Michaelis–Menton equation. Appl Math Lett 7:45–48
15. Adomian G (1995) Solving the mathematical models of neurosciences and medicine. Math Comput Simul 40:107–114
16. Wazwaz AM, Gorguis A (2004) An analytic study of Fishers equation by using Adomian decomposition method. Appl Math Comput 154:609–620
17. Loghambal S, Rajendran L (2013) Analytical expressions for steady-state concentrations of substrate and oxidized and reduced mediator in an amperometric biosensor., Int J Electrochem. doi: https://doi.org/10.1155/2013/812856
18. He JH (2006) Exp-function method for nonlinear wave equations. Chaos Solitons Fractals 30:700–708
19. Rajendran L, Anitha S (2013) Reply to "Comments on analytical solution of amperometric enzymatic reactions based on homotopy perturbation method," by Ji-Huan He, Lu-Feng Mo [Electrochim. Acta (2013)]., Electrochim Acta 102:474–476
20. Liu Z-J, Adamu MY Enoch S ,J-H He (2017) Hybridization of homotopy perturbation method and Laplace transformation for the partial differential equations. Thermal Sci 21(4):1843–1846
21. Adamu MY, Ogenyi P (2017) Parameterized homotopy perturbation method. Nonlinear Sci Lett A 8(2):240–243
22. He JH (1999) Homotopy perturbation technique. Comput Methods Appl Mech Eng 178:257–262
23. Ganesan S, Anitha A, L Rajendran (2013) Mathematical modeling of a carrier-Mediated transport process in a liquid membrane. J of Membrane Biol 246:435–442
24. Rasi M, Rajendran L, Sangaranarayanan MV (2015) Enzyme catalyzed oxygen reduction reaction in biofuel cells: Analytical expressions for chrono amperometric current densities. J Electrochem Soc 162(9):H671-H680